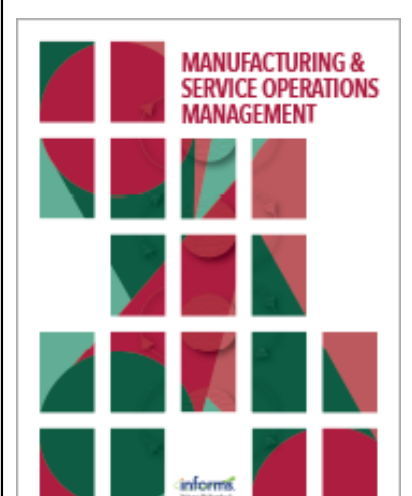
This article was downloaded by: [146.151.118.30] On: 31 August 2020, At: 07:14 Publisher: Institute for Operations Research and the Management Sciences (INFORMS) INFORMS is located in Maryland, USA



# Manufacturing & Service Operations Management

Publication details, including instructions for authors and subscription information: <a href="http://pubsonline.informs.org">http://pubsonline.informs.org</a>

# Charging an Electric Vehicle-Sharing Fleet

Long He, Guangrui Ma, Wei Qi, Xin Wang

#### To cite this article:

Long He, Guangrui Ma, Wei Qi, Xin Wang (2020) Charging an Electric Vehicle-Sharing Fleet. Manufacturing & Service Operations Management

Published online in Articles in Advance 03 Apr 2020

. https://doi.org/10.1287/msom.2019.0851

Full terms and conditions of use: <a href="https://pubsonline.informs.org/Publications/Librarians-Portal/PubsOnLine-Terms-and-Conditions">https://pubsonline.informs.org/Publications/Librarians-Portal/PubsOnLine-Terms-and-Conditions</a>

This article may be used only for the purposes of research, teaching, and/or private study. Commercial use or systematic downloading (by robots or other automatic processes) is prohibited without explicit Publisher approval, unless otherwise noted. For more information, contact permissions@informs.org.

The Publisher does not warrant or guarantee the article's accuracy, completeness, merchantability, fitness for a particular purpose, or non-infringement. Descriptions of, or references to, products or publications, or inclusion of an advertisement in this article, neither constitutes nor implies a guarantee, endorsement, or support of claims made of that product, publication, or service.

Copyright © 2020, INFORMS

Please scroll down for article—it is on subsequent pages



With 12,500 members from nearly 90 countries, INFORMS is the largest international association of operations research (O.R.) and analytics professionals and students. INFORMS provides unique networking and learning opportunities for individual professionals, and organizations of all types and sizes, to better understand and use O.R. and analytics tools and methods to transform strategic visions and achieve better outcomes.

For more information on INFORMS, its publications, membership, or meetings visit http://www.informs.org

### **MANUFACTURING & SERVICE OPERATIONS MANAGEMENT**



Articles in Advance, pp. 1–17

ISSN 1523-4614 (print), ISSN 1526-5498 (online)

# Charging an Electric Vehicle-Sharing Fleet

Long He,<sup>a</sup> Guangrui Ma,<sup>b</sup> Wei Qi,<sup>c</sup> Xin Wang<sup>d</sup>

<sup>a</sup> NUS Business School, National University of Singapore (NUS), Singapore 119245; <sup>b</sup> Antai Collage of Economics and Management, Shanghai Jiao Tong University, 200030 Shanghai, China; <sup>c</sup> Desautels Faculty of Management, McGill University, Montreal, Quebec H3A 1G5, Canada; <sup>d</sup> Department of Industrial and Systems Engineering and Grainger Institute for Engineering, College of Engineering, University of Wisconsin–Madison, Madison, Wisconsin 53706

Contact: longhe@nus.edu.sg, 🕞 http://orcid.org/0000-0002-9951-7450 (LH); guangrui.ma@sjtu.edu.cn,

http://orcid.org/0000-0002-2286-2571 (GM); wei.qi@mcgill.ca, lohttp://orcid.org/0000-0003-3948-835X (WQ); xin.wang@wisc.edu, http://orcid.org/0000-0003-3948-835X (WQ); xin.wang@wisc.edu,

Received: August 14, 2018 Revised: June 13, 2019; August 24, 2019 Accepted: September 7, 2019 Published Online in Articles in Advance: April 3, 2020

https://doi.org/10.1287/msom.2019.0851

Copyright: © 2020 INFORMS

Abstract. Problem definition: Many cities worldwide are embracing electric vehicle (EV) sharing as a flexible and sustainable means of urban transit. However, it remains challenging for the operators to charge the fleet because of limited or costly access to charging facilities. In this paper, we focus on answering the core question—how to charge the fleet to make EV sharing viable and profitable. Academic/practical relevance: Our work is motivated by the setback that struck San Diego, California, where car rental company car2go ceased its EV-sharing operations. We integrate charging infrastructure planning and vehicle repositioning operations that were often considered separately. More interestingly, our modeling emphasizes the operator-controlled charging operations and customers' EV-picking behavior, which are both central to EV sharing but were largely overlooked. Methodology: Supported by the real data of car2go, we develop a queuing network model that characterizes how customers endogenously pick EVs based on energy levels and how the operator implements a charging-up-to policy. The integrated queuing-location model leads to a nonlinear optimization program. We then propose both lower and upper bound formulations as mixed-integer second-order cone programs, which are computationally tractable and result in a small optimality gap when the fleet size is adequate. Results: We learn lessons from the setback of car2go in San Diego. We find that the viability of EV sharing can be enhanced by concentrating limited charger resources at selected locations. Charging EVs either in a proactive fashion or at the 40% recharge threshold (rather than car2go's policy of charging EVs only when their energy level drops below 20%) can boost the profit by more than 15%. Moreover, sufficient charger availability is crucial when collaborating with a public charger network. Increasing the charging power relieves the charger resource constraint, whereas extending per-charge range or adopting unmanned repositioning improves profitability. Finally, we discuss how EV sharing operations depend on the urban spatial structure, compared with conventional car sharing. Managerial *implications*: We demonstrate a data-verified and high-granularity modeling approach. Both the high-level planning guidelines and operational policies can be useful for practitioners. We also highlight the value of jointly managing demand fulfillment and EV charging.

Funding: This work was supported by the National Science Foundation [CNS Award 1637772], Fonds de Recherche du Québec-Société et Culture [Grant 267792], the National Natural Science Foundation of China [Grants 71602142, 91646118, and 91746210], the National University of Singapore [Start-Up Grant R-314-000-106-133], and the Natural Sciences and Engineering Research Council of Canada [NSERC Grant RGPIN-2019-04769].

Supplemental Material: The online appendices are available at https://doi.org/10.1287/msom.2019.0851.

Keywords: smart city operations • electric vehicles • car sharing • charging infrastructure

#### 1. Introduction

One of the building blocks for a smart city future is an electrified and shared mobility system. Such a system provides flexible on-demand transit services using a pool of electric vehicles (EVs). One representative business practice is the car-sharing service of car2go, a car rental company that runs Smart Fortwo EV fleets in cities such as Amsterdam and Madrid. Car2go members can pick up an available EV nearby, drive it

for a trip, and drop it off anywhere with signage on the street within its service region. This EV-sharing business model is gaining momentum worldwide, attracting market entrants including Volkswagen in Europe, Shouqi in China, and Communauto in Canada. Meanwhile, local governments, such as those of Singapore, Amsterdam, and Columbus, Ohio, also highlight the promotion of electrified and shared mobility in their race to launch smart city initiatives.<sup>1</sup> Electrified and shared mobility is widely expected to prevail because of two driving forces. First, economic restructuring, in the form of the booming sharing economy along with online/offline service integration, has its largest impact on the transportation sector. Global Market Insights (2018) projects that the global revenue of the car sharing industry will rise to \$12 billion by 2024. Second, stringent environmental regulations on emissions spur vehicle electrification by phasing out fossil-fuel vehicles. For example, the United Kingdom and France will prohibit the sale of new internal-combustion cars by 2040, India has set its deadline to 2030, and China is working on its timetable for a similar mandate (Condliffe 2017).

Nonetheless, a smart EV-sharing system cannot be built in one day. A recent setback occurred in San Diego, where car2go ceased operations of its EV-sharing fleet in 2016. The *San Diego Union-Tribune* reported the EV-sharing operator's reason:

We're just not able to keep the cars charged, and people aren't able to charge them on their own.... We just don't have the infrastructure we need here to make it work now. (Dacyl Armendariz, car2go spokesperson, quoted in Garrick 2016)

Indeed, insufficient charging causes low battery energy levels and thus limited availability of EVs to fulfill travel demands, which can ultimately throttle the operation. To tackle this issue, EV-sharing operators face grand challenges:

- At the strategic level, unlike sharing conventional fossil-fuel vehicles, EV sharing crucially depends on the infrastructure for battery charging. Unfortunately, such infrastructure is often scarce. For example, in 2011, a federally subsidized nonprofit, ECOtality, promised it would install 1,000 Blink chargers in San Diego. However, only about 400 were installed when car2go finally stopped doing business (Garrick 2016). Moreover, those 400 public chargers were only partially available to car2go while accommodating competing charging demands from other EV owners. Given the high construction cost of charging infrastructure and its scarcity, it is imperative to carefully decide the locations and quantities of chargers to install
- At the operational level, the EV-sharing operator has to conduct intertwined repositioning and battery charging operations to meet travel demand. Unbalanced customer trips often lead to either too few or excessive EVs at some locations. It is thus important for the operator to reposition EVs to improve vehicle utilization by meeting more demands at more locations. However, the repositioning of EVs is much more challenging than that of fossil-fuel vehicles—EVs take significantly longer charge time yet with shorter per-charge range. The energy remaining in the battery,

hereafter referred to as the *energy level*, is critical to demand fulfillment and the feasibility of repositioning. A salient feature of EV sharing is that the energy levels of vehicle flows should be closely tracked to ensure charging EVs timely, as well as to improve demand fulfillment.

We try to address these challenges by proposing models, analytics, and insights for designing a better EV-sharing system. The objective is to satisfy urban mobility demands in a shared and electrified fashion while maximizing the revenue net of the infrastructure investment and operating cost. Our paper presents an integrated model to jointly determine the locations and sizes of battery charging sites, along with the coupled fleet charging and repositioning operations. Through a case study based on real data, we aim to understand whether car2go could have performed better. More important, we provide managerial insights into the future development of EV sharing for cities and companies that pursue this mobility paradigm. We briefly summarize the contributions of this paper as follows:

- 1. To the best of our knowledge, this work is the first attempt to provide models to jointly plan and operate an EV-sharing system, with an emphasis on high-granularity modeling of energy-level-indexed EV flows, endogenous customers' EV-picking behavior, and the operator's charging operations. These operational aspects are central to EV sharing but have been overlooked at the network scope in the literature.
- 2. Our work also demonstrates a *data-verified* modeling approach. We rely on real data and empirical evidence to guide our modeling process (e.g., EV arrival and departure processes, customers' EV-picking behavior, and the operator's charging policy). Our demand recovery method helps correct observational bias from the censored data. Collectively, our model and managerial insights can be of practical value to EV-sharing practitioners.
- 3. We propose a new solution technique to tackle the resulting optimization model—a nonlinear program with fractional constraints (involving quadratic denominators). Our lower and upper bound solutions can be obtained by solving mixed-integer second-order cone programs (MISOCPs). The bounds result in small optimality gaps (for cases with adequate fleets), allowing efficient computation and significantly more straightforward implementation than the branch-and-bound solution techniques in the literature.
- 4. By examining car2go operations from computational studies on real data, we provide managerial insights to help launch future EV-sharing programs:
- Contrary to car2go's practice of charging EVs only at energy levels below 20%, car2go should, ideally, proactively charge EVs from varying energy levels contingent on the operational status of the entire

system. Alternatively, a more implementable adjustment is to increase the charging activation threshold to 40% (with reoptimized charging infrastructure). Furthermore, its fleet size may be reduced by up to 20% without incurring significant profit loss.

- Ensuring sufficient charger availability is crucial when collaborating with a public charger network. When the availability of the public chargers is low, the EV-sharing service provider should consider installing private chargers to ensure timely access to energy at optimal locations.
- Various EV technological advancements lead to different performance improvements. Elevating charging power relieves the charger resource constraint, thus enhancing the business viability in the early stage. By contrast, extending the per-charge range or adopting unmanned repositioning improves profitability, thus being favorable in the long run.
- Finally, EV sharing also differs from conventional car sharing in how its profitability and operations depend on the urban spatial structure. A more centralized customer trip pattern (into and out of a central business district) can be favorable to EV sharing because the savings from charging operations and investment may dominate the expenditure on rebalancing supply/demand.

The remainder of this paper is organized as follows. Section 2 reviews the related literature. Section 3 describes the optimization model of planning and operating an EV-sharing system. Section 4 develops tractable formulations to obtain lower and upper bounds for the optimal profit. Section 5 presents the case study and managerial insights into the future development of EV sharing. Finally, Section 6 concludes the paper. A summary of notations, additional proofs, formulations, and results are available in the online appendices.

Throughout the paper, we denote sets by calligraphic uppercase English letters, system parameters by lowercase English letters, vehicle flow decision variables and service levels by lowercase Greek letters, and other decision variables by uppercase English letters.

#### 2. Literature Review

Infrastructure planning for shared and electrified mobility is essential to the development of smart cities but has drawn little attention in the literature. The majority of the literature on vehicle-sharing service systems considers vehicles without battery charging concerns (e.g., fossil-fuel cars and bikes). For one-way mobility sharing, a main operational challenge is that the operators have to proactively reposition their fleets to maintain a certain service level in the presence of spatially asymmetric trip demands. Recent studies have made some progress in this direction. At

the strategic level, Kabra et al. (2018) develop a structural choice model to empirically analyze the impacts of accessibility of stations and the availability of vehicles in a bike-sharing system. Lu et al. (2017) consider the problem of allocating parking lots or permits in joint with fleet repositioning operations. Similarly, Kaspi et al. (2014, 2016) study parking reservation policies and regulations. At the operational level, Adelman (2007) develop a queuing network to study the rail equipment repositioning problem. Nair and Miller-Hooks (2011) consider a vehicle repositioning problem with service-level constraints. Shu et al. (2013) solve a bike redistribution network flow problem. Benjaafar et al. (2018) and He et al. (2020) propose different approaches to solving the stochastic dynamic rental product or vehicle repositioning problems. However, those one-way mobility-sharing models cannot be directly applied to EV-sharing fleets because the battery charging operations are absent. As implied by the failure of car2go in San Diego, managing charging operations is critical to the success of the EVsharing business.

Our paper aims to address several obstacles that arise from electrifying car-sharing systems, including planning battery charging infrastructure, managing coupled charging and repositioning operations, and estimating travel demand. Among few related studies, Boyacı et al. (2015) build a planning model to analyze station-based EV sharing, considering station location, parking space allocation, fleet size management, and vehicle relocation. He et al. (2017) propose a mathematical programming model to solve for the optimal service region planning for EV sharing, incorporating customer subscription decisions and fleet operations. By considering an aggregated market without heterogeneities across locations and EVs, Abouee Mehrizi et al. (2018) develop an analytical model to discuss the viability of using EVs in a car-sharing system. However, those papers abstract away detailed operations that are critical to EV sharing such as, for example, endogenized customers' EV-picking behavior and the operator's EV charging management.

Among those papers, He et al. (2017) is the closest to ours. Nevertheless, they do not consider heterogeneous energy levels of EVs and simply assume that 20% of all EVs arriving at each location enter the charging process and that all EVs available for customers are fully charged. Moreover, they consider demand fulfillment as a centralized decision by the operator. By contrast, our model incorporates energy-level tracking, heterogeneous and stochastic charging durations of EVs, and how customers pick EVs based on available energy levels under the range anxiety studied in Lim et al. (2015) and observed empirically in Kim et al. (2018). These considerations are realistic

but novel to the literature, resulting in a high-granularity characterization of EV-sharing operations. Moreover, those papers implicitly assume that charging facilities are available at all locations. In reality, charging facilities are scarce and costly to build in the early stage of this business, which our model explicitly addresses.

Finally, our paper also relates to the literature on EV-related service planning and operations management in the conventional nonsharing contexts. For instance, Mak et al. (2013) apply robust optimization to solve for battery-swapping locations along highways to accommodate exogenous EV flows. Our modeling of the plug-in battery-charging process is novel and fundamentally different from that of battery swapping, which requires negligible time. Lim et al. (2015) compare potential mass EV adoption under different business settings (e.g., selling and leasing) with consumer anxieties about the range and resale of EVs. Jiang and Powell (2016) propose a riskaverse Markov decision process model for dynamically charging EVs in the presence of electricity spot price variations. Zhang et al. (2018) address the coupling between transportation and electrical grid networks when planning EV charging facilities. The charging requirement also brings new challenges to freight logistics services when employing EVs. Schneider et al. (2014) and Desaulniers et al. (2016) formulate EV routing problems with charging schemes under timewindow constraints and propose-optimization algorithms. The key distinction of our work from those papers is the explicit characterization of the coupled charging and repositioning operations as well as the distributions of EV energy levels, which are central in the EV-sharing context.

# 3. EV-Sharing System Planning and Operations

We model the fleet operations in the EV-sharing system using a queuing network. Planning charging infrastructure includes charging site selection and charger installation, which configures the network. We use binary decision variable  $X_i$  to denote whether the operator deploys any charger in zone  $i \in \mathcal{I}$ , where  $\mathcal{I}$  is the set of zones that form the service region. At selected site i (i.e.,  $X_i = 1$ ), the operator further specifies the number of chargers  $Y_i$ .

We consider a multiclass open queuing network consisting of single-server nodes for the demand zones, infinite-server nodes for the roads, and multiserver nodes for the charging sites. Constructed from a vehicle's perspective, EVs are viewed as the entities in the queuing network. We briefly explain each type of node and its connections before the detailed discussions in the following subsections.

• Each demand zone is considered as a single "server." An "arrival" event indicates that an EV is

dropped off in a zone, and a "departure" event indicates that an EV leaves a zone. The available EVs that wait in zone i will be picked up by customers at the service rate that is endogenously determined by the demand rate and customers' EV-picking behavior. Note that EVs are differentiated by their energy levels, and customers tend to pick available EVs with the highest energy. Thus, each demand node is modeled as a multiclass M/M/1 queue with preemptive-repeat priority and class-dependent service rates in Section 3.2.

- The roads are modeled as  $M/G/\infty$  nodes with generally distributed travel times, because EVs leaving a demand zone can immediately get on the road (enter "service"). We choose to model the transit traffic using an infinite-server queue because it has been discussed in various settings for traffic on a long road with free overtaking (Daley 1976) and also commonly used in vehicle sharing studies (e.g., George and Xia 2011, He et al. 2017).
- The charging node in zone i, if available, is represented by an  $M/G/Y_i$  queue where  $Y_i$  specifies the number of chargers. Its service time distribution depends on the specific charging policy, which we will analyze in Section 3.3 under a charging-up-to policy motivated by the data.
- Nodes in the network interact with each other through the movements of vehicles. Instead of using a closed queuing network, our model "loosely" connects all nodes by the mean flow balance in each node and the expected total fleet size in the system for the practicality and tractability reasons. First, in reality, the number of EVs in the system is not always constant. We characterize the expected total fleet size as the system's capacity. Second, although the closed queuing networks in George and Xia (2011) and He et al. (2017) preserve product-form solutions, it is not the case in our problem. In those papers, all vehicles are homogeneous, and thus their networks only consist of infinite-server nodes with generally distributed service times and single-server nodes with exponential service times, which fall into the class of BCMP (Baskett, Chandy, Muntz and Palacios) networks (Baskett et al. 1975). Our challenge here is that EVs are nonidentical by their energy levels, which prohibits use of the BCMP network. Nonetheless, it is realistic and important to explicitly differentiate EVs by energy level in this study. In Section 3.4, we discuss the interaction among nodes and the integration of all modeling components into an optimization model.

The key assumption underlying the queuing network is the Poisson vehicle arrivals and departures, which have been widely adopted to model vehicular flows (e.g., Freund et al. 2019 in bike sharing). In what follows, we first examine this assumption using an operational data set from car2go in San Diego.

#### 3.1. Poisson Vehicle Arrivals and Departures

We collected one-month records of EVs within the entire service region of 16 zip code areas (as zones) every five minutes from car2go in March 2014. The attributes recorded include time stamps, location coordinates, battery energy levels, and charging status (i.e., being charged or not) for each idle EV. For the purpose of this study, we translate the time-stamped data into trip-level data. We identify 19,380 trips (with travel times longer than 10 minutes) with origins and destinations, energy consumption, and travel times.

We conduct statistical testing for the Poisson vehicle arrival and departure assumption for the entire system instead of individual zones because the sample sizes become too small for each zone at the hourly level. We set up the tests following Kim and Whitt (2014), who examine the classical conditional uniform property of Poisson process. That is, conditional on the number of arrivals (departures) n in any interval, the n-ordered arrival (departure) times are independently and identically distributed random variables with uniform distribution along the interval. Because the trip records are time stamped at every five minutes, the recorded customer arrival (departure) time (i.e., the trip start (end) time) is not continuous. Therefore, we construct tests for the discrete uniform distribution.

We start by visualizing the arrival and departure time stamps of EVs in the entire system. Figure 1 shows the histograms of the time stamps within each hour. Because the trip records are at the five-minute granularity, the bin size in the histograms is also set to be five minutes. Note that most of the bins have similar heights for both arrivals and departures.

To statistically test for the discrete uniform distribution, we consider all one-hour intervals over 25 days in the trip data. Suppose that  $n_{hq}$  arrivals occurred during hour h on day q. The trip start times  $t_{hq}^{j}$ ,  $\forall j \in$ 

 $\{1, \dots, n_{hq}\}$  are hypothesized to follow the discrete uniform distribution among all 12 distinct time stamps (at the five-minute level) in the interval. Each time stamp is then viewed as a bin, and the number of trips in the bin is counted as  $z_{hq}^k$ ,  $\forall k \in \{1, \dots, 12\}$ . Therefore, we formulate the null hypothesis as follows:  $z_{hq}^k$ ,  $\forall k \in$  $\{1, \cdots, 12\}$  follows the discrete uniform distribution with probability mass function  $\frac{1}{12}$ . In our data set, a total of 275 one-hour intervals over 25 days have trip sample sizes larger than 50. We only conduct hypothesis tests for those intervals to ensure the accuracy of Pearson's  $\chi^2$  test. Because 94.5% of the tests report p-values larger than 0.05, the uniform arrivals hypothesis is *not* rejected. Similarly, we apply the test to departure time stamps, where 93.5% of the tests report p-values larger than 0.05. Consequently, we do *not* reject the uniform departure hypothesis either. Hence, the test suggests that the Poisson assumption is reasonable for both vehicle arrivals and departures.

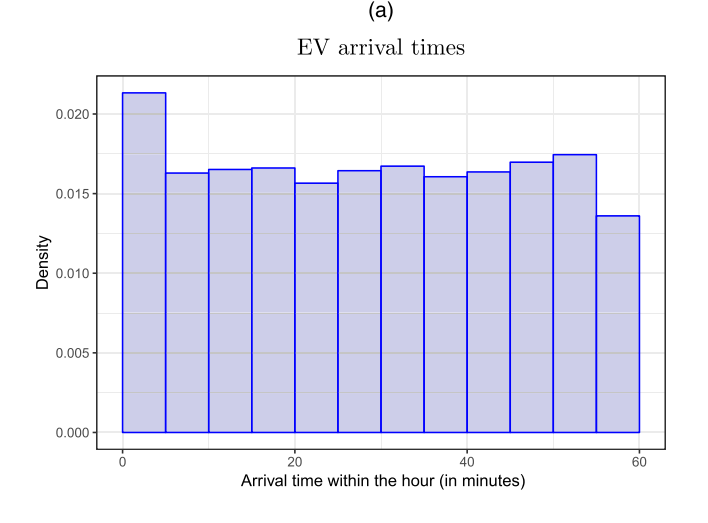
Furthermore, the data suggest that customer demand rates vary over time. To incorporate the system dynamics, we divide a day into multiple periods and employ the point-wise stationary approximation approach in Green and Kolesar (1991) such that the customer demands are considered stationary within each period. Based on the travel intensity, we divide a day into five periods and summarize the average trip rate, energy consumption, and travel time in Table 1. The detailed multiperiod optimization formulation is provided in Online Appendix B and used in our case study in Section 5. For ease of exposition, we present the modeling of the EV-sharing system in a single period.

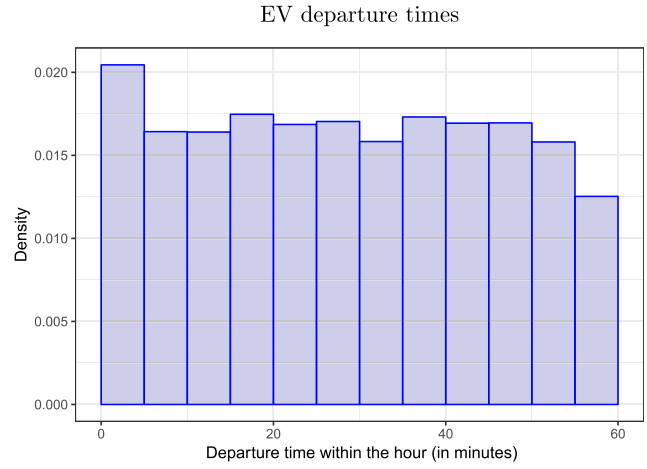
### 3.2. Customers' EV Picking

From an EV-sharing operator's perspective, it is important to understand how customers choose EVs to

(b)







| Period           | Hourly trip rate | Per-trip energy consumption (kWh) | Travel time (in minutes) |
|------------------|------------------|-----------------------------------|--------------------------|
| 7 a.m.–9:59 a.m. | 38.57            | 1.19                              | 32.82                    |
| 10 a.m12:59 p.m. | 39.93            | 1.20                              | 31.29                    |
| 1 p.m3:59 p.m.   | 45.12            | 1.19                              | 27.15                    |
| 4 p.m6:59 p.m.   | 48.74            | 1.34                              | 27.36                    |
| 7 n m 6:50 a m   | 17.2             | 1 28                              | 33.50                    |

**Table 1.** Average Hourly Customer Trip Rate, Energy Consumption per Trip, and Travel Time per Trip

fulfill their travel needs. For this purpose, we first distinguish EVs by their energy levels. Specifically, we use e to label the energy levels of EVs and discretize the range of energy levels into a finite set  $\mathscr{E} = \{0,1,\ldots,\bar{e}\}$ , where  $\bar{e}$  is the highest energy level. That is, we can map the actual battery levels into the discretized energy levels. For example, if the battery capacity is 20 kWh and  $\bar{e} = 10$ , one unit of energy level represents 2 kWh. Online Appendix A provides a table of key notations in this paper.

In EV-sharing systems, customers usually have access to the energy-level information of EVs through the website or mobile applications. A customer to travel from zone i to zone j will seek in zone i an available EV that has at least  $e_{ij}$  amount of energy remaining, where  $e_{ij}$  is the energy consumed by a customer trip from i to j. If there is no available EV or all available EVs do not have sufficient energy (i.e.,  $e < e_{ij}$ ) in zone i, the demand will be lost. Otherwise, there are three potential modes of customer EV-picking behavior:

- 1. The "indifference" mode assumes that the customer will randomly pick up an EV among the available ones with sufficient energy.
- 2. The "angel" mode assumes that the customer will choose the EV with the least (yet sufficient) amount of energy so as to leave EVs with higher energy levels to other customers.
- 3. The "risk-averse" mode assumes that the customer will choose the EV with the highest energy level to minimize the risk of battery depletion before the trip ends.

We choose to model the customers' EV-picking behavior based on the risk-averse mode. First, the risk-averse mode is empirically verified. Kim et al. (2018) observe that in car2go San Diego, EV range anxiety impelled EV-sharing customers to strictly prefer higher energy levels to lower ones. Second, from the operator's perspective, the risk-averse mode is more conservative to assume than the other two modes. The resulting charging and repositioning schemes are reliable even if the realized customers' EV-picking behavior may deviate from such an assumption. Third, the assumption of the risk-averse mode admits tractable modeling of the demand-fulfillment process with high granularity. By contrast, it is challenging to integrate the other two behavioral modes into our model, which we leave for future research.

With the risk-averse mode of EV picking, the demandfulfillment process becomes highest-energy-first-out (HEFO), as shown in Figure 2, which allows us to model it as a multiclass M/M/1 queue with preemptiverepeat priority and class-dependent service rates. Specifically, recall that zone *i* is a "server," whose service rate depends on the energy levels of the available vehicles. The service rate for an EV with energy level *e* is  $\hat{d}_{ie} = \sum_{j \in \mathcal{J}_{ie}} d_{ij}$ , where  $d_{ij}$  is the demand rate for trips from zone *i* to zone *j* and  $\mathcal{J}_{ie} = \{j : e_{ij} \leq e\}$  is the set of destinations reachable by energy level *e* from origin *i*. Suppose that we divide all EVs into  $\bar{e}$  classes according to their energy levels (i.e., class e for EVs with energy level e). Under the risk-averse mode, an EV can be "served by zone i" only when all EVs of higher class (i.e., with higher energy levels) have been taken, which clearly suggests the preemptive priority rule class  $\bar{e}$  has the highest priority and class 0 has the lowest priority.

Let  $\psi_{ije}$  be the fulfilled demand rate for customers traveling from i to j using EVs with energy level e. The load of class e can be defined as

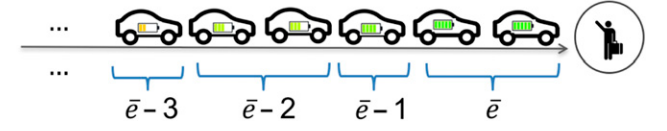
$$\alpha_{ie} = \frac{\sum_{j \in \mathcal{J}_{ie}} \psi_{ije}}{\hat{d}_{ie}} \tag{1}$$

for zone *i*. Furthermore, because customers are not required to inform the operator about their destinations, the operator is not able to ration the demand to fulfill by trip destinations. Therefore, the satisfied customer trips follow the proportional rule as

$$\psi_{ije} = \frac{d_{ij}}{\hat{d}_{ie}} \sum_{i \in \mathcal{I}_{ie}} \psi_{ije}, \forall j \in \mathcal{J}_{ie}.$$
 (2)

We next express the expected queue lengths for EVs with different energy levels in zone i in terms of the load  $\alpha_{ie}$ . We apply the queue-length formula for the multiclass M/G/1 queue with preemptive priority in

**Figure 2.** (Color online) EV Picking by "Risk-Averse" Customers with Range Anxiety



Shortle et al. (2018). Note that this formula is derived under the assumption that interrupted entities resume "service" from the point of interruption. In our setting, however, the interrupted (lower-energy) EVs start over the "service" after the interruption in the demand zone. Nevertheless, given the exponential service time, this discrepancy is irrelevant in view of the memoryless property (Shortle et al. 2018). Hence, with the mean  $\frac{1}{d_{le}}$  and the second moment  $\frac{2}{d_{le}^2}$  of the exponential service time of class e, the average number (queue length) of EVs with energy level e in zone i is given by

$$L_{ie} = \frac{\alpha_{ie} \left[ 1 - \sum_{e'=e}^{\bar{e}} \alpha_{ie'} + \hat{d}_{ie} \sum_{e'=e}^{\bar{e}} \frac{\alpha_{ie'}}{\hat{d}_{ie'}} \right]}{\left( 1 - \alpha_{i\bar{e}} - \alpha_{i(\bar{e}-1)} - \dots - \alpha_{i(e+1)} \right)}, \quad \forall e < \bar{e}, \quad (3)$$

$$\left( 1 - \alpha_{i\bar{e}} - \alpha_{i(\bar{e}-1)} - \dots - \alpha_{ie} \right)$$

$$L_{i\bar{e}} = \frac{\alpha_{i\bar{e}}}{1 - \alpha_{i\bar{e}}}. (4)$$

#### 3.3. Charging Process

The operator also needs to closely monitor the EV charging process, which is central to the availability of EVs. To focus on a practical charging process, we begin this subsection by analyzing the energy levels of EVs in the car2go data. In the data set, as described in Section 3.1, we identify 1,472 trips that went through a charging process with at least a 10% energy level increase. We present their energy-level distributions(in percent) on entering and leaving a charging process in Figure 3.

Car2go sets a recharge threshold at the 20% energy level, under which an EV must be moved to charge. Figure 3(a) shows that the energy levels of most EVs when entering a charging process are around this threshold. Occasionally, EVs with an energy level higher than 20% can also be sent to charge. We refer to car2go's practice as a *threshold-activated* charging policy. By contrast, we consider a *proactive* charging policy where the operator can choose to charge EVs with different energy levels (lower than  $\bar{e}$ ).

After discussing when to charge EVs, we examine when to finish charging. Figure 3, (b)–(d), shows the energy levels of EVs departing from a charging process. These histograms suggest that the energy levels after charging could depend on location. As implemented by car2go, EVs can be charged to 50% or 100% before being released from the charging sites. These observations motivate us to study a *charge-up-to policy* to reflect car2go's practice. That is, the operator charges all EVs to energy level  $\bar{e}$ . For ease of exposition, we consider a single parameter  $\bar{e}$ —that is, the highest energy level. In practice,  $\bar{e}$  can potentially vary by time

or location (which a direct extension of our model can capture).

We model such a charging process at each site i with  $Y_i$  chargers as an  $M/G/Y_i$  queue. Under the proactive charge-up-to policy, the EVs that arrive with energy level e follow a Poisson process with rate  $\lambda_{ie}$  (which is controlled by the operator), and the charging time is  $\frac{\bar{e}-e}{u}$ , where u denotes the charging power. Therefore, the charging time of any EV follows a discrete distribution, being  $\frac{\bar{e}-e}{u}$  with probability  $\frac{\lambda_{ie}}{\sum_{e<\bar{e}}\lambda_{ie}}$ , with mean  $a_i = \sum_{e<\bar{e}}\frac{\bar{e}-e}{u}\frac{\lambda_{ie}}{\sum_{e<\bar{e}}\lambda_{ie}}$  and variance  $b_i^2 = \sum_{e<\bar{e}}\frac{(\bar{e}-e)^2}{u^2}\frac{\lambda_{ie}}{\sum_{e<\bar{e}}\lambda_{ie}} - a_i^2$ . Then we approximate the expected waiting time in the queue (excluding the charging time)  $W_i^q$  by using the heavy-traffic formula from Whitt (1993) as follows:

$$\mathbb{E}[W_i^q] = \frac{\rho_i a_i}{Y_i (1 - \rho_i)} \frac{c_a^2 + c_s^2}{2},$$

where the utilization ratio  $\rho_i = \frac{a_i \sum_{c < \bar{c}} \lambda_{ic}}{Y_i}$ ,  $c_s^2 = \frac{b_i^2}{a_i^2}$ , and  $c_a^2 = 1$ . The heavy-traffic approximation is asymptotically accurate as  $\rho_i$  approaches 1. Such approximation is particularly appropriate in our setting, where the charging resources, either constrained in car2go's practice or optimized in our solution, are heavily utilized. In fact, for all the numerical instances in Section 5, the values of  $\rho_i$  are sufficiently high (above 0.96) in the peak period (when the fleet size constraint is binding, and this formula is relevant). Note that we choose not to use the alternative heavytraffic approximation from Kingman (1965),  $\frac{a_i(\frac{1}{p_i}+\rho_ic_s^2)}{2Y_i(1-\rho_i)}$ which is more common in the literature (e.g., Shortle et al. 2018). This alternative formula would be structurally less tractable in the optimization model in Section 3.4, and it would only negligibly improve the accuracy given the close-to-one  $\rho_i$  in our setting.

Therefore, the expected time an EV spends at site *i*, including both the time in the queue and the time being charged, is given by

$$\begin{split} \mathbb{E}[W_i] = & \mathbb{E}\big[W_i^q\big] + a_i = \frac{\sum_{e < \bar{e}} \frac{(\bar{e} - e)^2}{u^2} \lambda_{ie}}{2Y_i^2 - 2Y_i \sum_{e < \bar{e}} \frac{\bar{e} - e}{u} \lambda_{ie}} \\ & + \sum_{e < \bar{e}} \frac{\bar{e} - e}{u} \frac{\lambda_{ie}}{\sum_{e < \bar{e}} \lambda_{ie}}. \end{split}$$

By Little's law, the expected number of vehicles  $Q_i$  at charging site i is given by

$$Q_{i} = \left(\sum_{e < \bar{e}} \lambda_{ie}\right) \mathbb{E}[W_{i}]$$

$$= \frac{\left(\sum_{e < \bar{e}} \lambda_{ie}\right) \sum_{e < \bar{e}} \frac{(\bar{e} - e)^{2}}{u^{2}} \lambda_{ie}}{2Y_{i}^{2} - 2Y_{i} \sum_{e < \bar{e}} \frac{\bar{e} - e}{e} \lambda_{ie}} + \sum_{e < \bar{e}} \frac{\bar{e} - e}{u} \lambda_{ie}.$$
 (5)

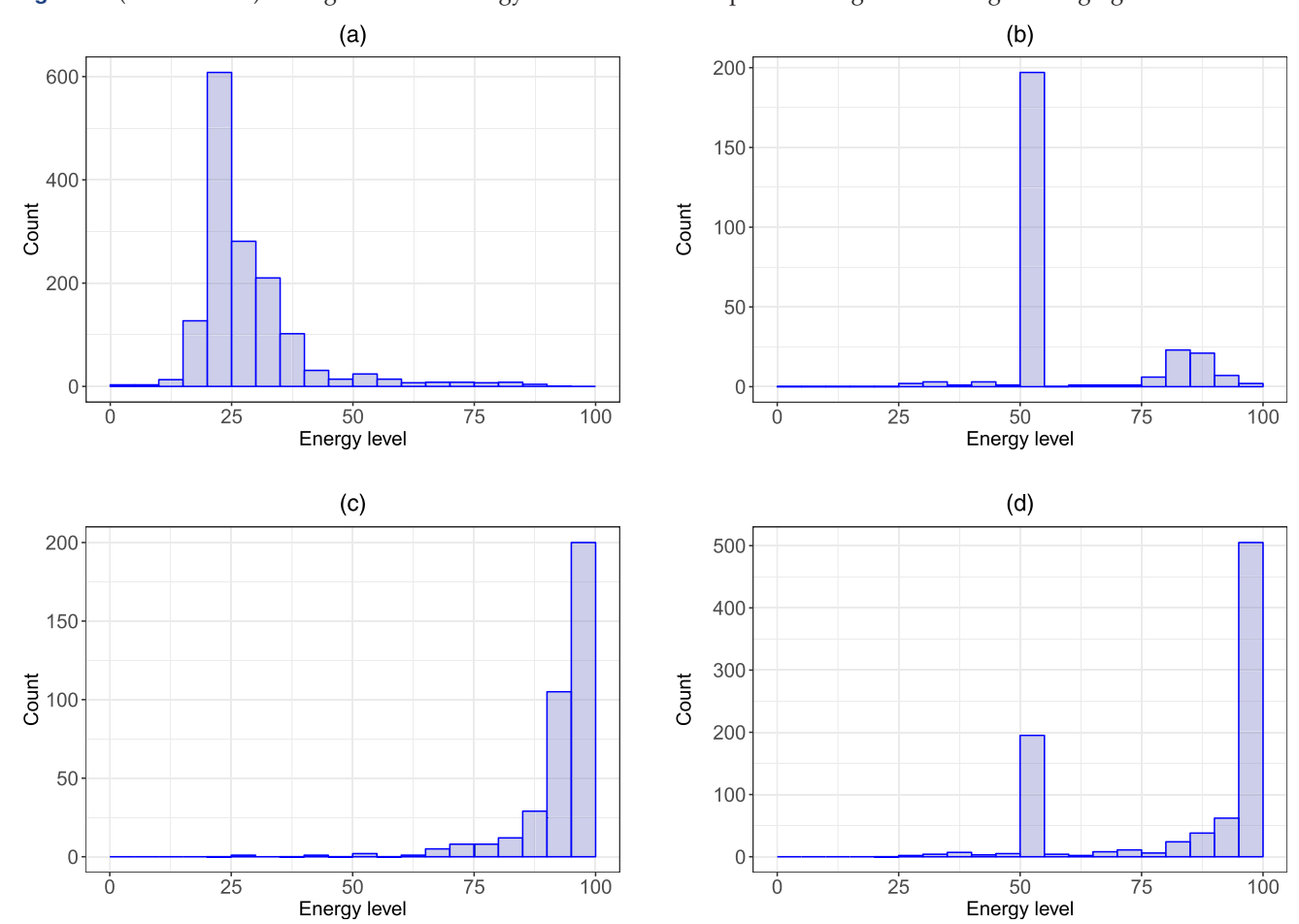


Figure 3. (Color online) Histogram of EV Energy Levels in Percent upon Entering and Leaving a Charging Process

Note. (a) Energy levels before charging in the entire system; (b) Energy levels after charging at zones 92105, 92109, and 92115 (by zip code); (c) Energy levels after charging at zones 92102, 92103, 92110, and 92116 (by zip code); (d) Energy levels after charging at zones 92101, 92106, 92107, and 92108 (by zip code).

Because the utilization ratio  $\rho_i \leq 1$ , we have

$$Y_i \ge \sum_{e < \bar{e}} \frac{\bar{e} - e}{u} \lambda_{ie}.$$
 (6)

#### 3.4. The Optimization Model

Having described the key features in EV sharing—namely, the customers' EV-picking behavior and the operator's charging-up-to policy—we develop an integrated optimization model for the design and operation of a system with m EVs.

Zooming out the view to the entire service region, the EV-sharing fleet moves across and within zones. EV movements consist of both transit trips by customers and repositioning trips by the operator, which we characterize as aggregated EV flows at different energy levels. As suggested by Section 3.1, we model

the transit trips from zone i to j with EVs at energy level e on departure as a Poisson process with rate  $\psi_{ije}$ . Because only those EVs with energy level  $e \geq e_{ij}$  are feasible for such a trip, we have  $\psi_{ije} = 0$  for  $e < e_{ij}$ . Moreover, to rebalance the system in the presence of asymmetric EV flows by customers, the operator needs to carry out repositioning trips from zone i to j with rate  $\phi_{ije}$  for EVs with energy level e. Suppose that an EV consumes  $e_{ij}^r$  energy for repositioning from zone i to j. We have  $\phi_{ije} = 0$  for  $e < e_{ij}^r$ . The operator also dispatches workers to move EVs within each zone: EVs with energy level  $e < \bar{e}$  enter the charging site in zone i (if open) with rate  $\lambda_{ie}$  and depart from the charging process with rate  $\eta_i$  after reaching energy level  $\bar{e}$ .

Under the Poisson assumption, the actual number of EV movements (e.g., customer and repositioning

trips) is stochastic. In practice, the operator can implement the repositioning by splitting Poisson EV flows (e.g., blocking a proportion of arrived EVs from customers for repositioning workers). With necessary repositioning, the operator maintains the balance of EVs at various energy levels in the system. The following *energy-flow balance equations* characterize the EV flows in each zone and in the charging sites:

$$\sum_{j \in \mathcal{I}} \left( \psi_{ji(e+e_{ji})} + \phi_{ji(e+e_{ji}^{r})} \right)$$

$$= \sum_{i \in \mathcal{I}} \left( \psi_{ije} + \phi_{ije} \right) + \lambda_{ie}, \quad \forall i \in \mathcal{I}, e \in \mathcal{E} \setminus \bar{e}, \tag{7}$$

$$\eta_{i} = \sum_{i \in \mathcal{I}} \left( \psi_{i\bar{j}\bar{e}} + \phi_{i\bar{j}\bar{e}} \right) + \lambda_{i\bar{e}}, \quad \forall i \in \mathcal{I},$$
 (8)

$$\eta_i = \sum_{e \in \mathcal{E}} \lambda_{ie}, \qquad \forall i \in \mathcal{I}. \tag{9}$$

The balance equations (7) and (8) trace the EV flows with energy levels  $e < \bar{e}$  and  $\bar{e}$ , respectively, for each zone *i*. In Equation (7), the term  $\sum_{j \in \mathcal{J}} (\psi_{ji(e+e_{ji})} + \phi_{ji(e+e_{ji})})$ summarizes the total EV inflows into zone *i*, whose energy level on arrival is e. The term on the right-hand side (RHS),  $\sum_{j \in \mathcal{I}} (\psi_{ije} + \phi_{ije}) + \lambda_{ie}$ , represents the total outflow from zone i by transit trips and repositioning trips for fleet rebalance and to the charging site at zone *i*. Note that this equation concerns EV inflows from other zones, and therefore, their energy levels are less than  $\bar{e}$ . For EVs with energy level  $\bar{e}$ , Equation (8) indicates that the inflow comes only from the charging site in zone *i* with rate  $\eta_i$ , and the term on the RHS,  $\sum_{i \in \mathcal{I}} (\psi_{i\bar{i}\bar{e}} + \phi_{i\bar{i}\bar{e}}) + \lambda_{i\bar{e}}$ , is the total EV outflow with energy level  $\bar{e}$ . The last equation (9) shows the flow balance at charging site *i*.

The above-mentioned energy-flow balance equations connect the flow variables—namely,  $\psi_{ije}$ ,  $\phi_{iie}$ ,  $\lambda_{ie}$ , and  $\eta_i$ . We next integrate the two features of EV sharing (i.e., the customers' EV-picking and operatorcontrolled charging processes) using a fleet size constraint. As modeled in Sections 3.2 and 3.3, the expected number of EVs that idle in zone i and stay at charging site i is given by  $L_{ie}$  and  $Q_i$  in Equations (3)–(5). To derive the expected numbers of EVs in another status (e.g., in transit by customers and repositioning by the operator), we apply Little's law. That is, the expected number of EVs traveling from zone *i* to *j* with initial energy level e is  $t_{ij}\psi_{ije}$  for customer transit and  $s_{ij}\phi_{iie}$  for repositioning, where  $t_{ij}$  and  $s_{ij}$  are the expected travel time in transit and repositioning between zones, respectively. Let  $s_{ii}$  be the expected travel time for EVs entering and leaving the charging sites. The expected number of EVs repositioned to and from the charging sites is given by  $s_{ii}(\sum_{e < \bar{e}} \lambda_{ie} + \eta_i)$ in zone i. The sum of all these EV quantities is no

larger than the fleet size *m*, which the following fleet size constraint imposes:

$$\sum_{i \in \mathcal{I}} \left( Q_i + \sum_{e \in \mathscr{E}} L_{ie} \right) + \sum_{i \in \mathcal{I}} \sum_{j \in \mathscr{I}} \sum_{e \in \mathscr{E}} \left( t_{ij} \psi_{ije} + s_{ij} \phi_{ije} \right) + \sum_{i \in \mathscr{I}} s_{ii} \left( \sum_{e < \bar{e}} \lambda_{ie} + \eta_i \right) \le m.$$
(10)

Let p be the revenue from customer usage per unit time per EV, let c be the repositioning cost per unit time per EV, let  $f_i$  be the fixed setup cost of a charging site in zone i, and let g be the installation cost per charger. Suppose that the maximum number of chargers allowed is  $\bar{y}_i$  in zone i. Recall that  $X_i \in \{0,1\}$  indicates whether to offer charging service, and  $Y_i \in \mathbb{R}^+$  indicates the number of chargers installed in zone i. We formulate the charging infrastructure planning and fleet operations problem for EV sharing as a nonlinear optimization problem (NLP):

$$\max_{\substack{X,Y,\phi,\psi\\\alpha,\lambda,\eta,L,Q}} p \sum_{i\in\mathcal{I}} \sum_{j\in\mathcal{I}} \sum_{e\in\mathcal{E}} t_{ij} \psi_{ije} - c \sum_{i\in\mathcal{I}} \sum_{j\in\mathcal{I}} \sum_{e\in\mathcal{E}} s_{ij} \phi_{ije}$$

$$-c \sum_{i\in\mathcal{I}} s_{ii} \left( \sum_{e<\bar{e}} \lambda_{ie} + \eta_i \right) - \sum_{i\in\mathcal{I}} (f_i X_i + g Y_i)$$
(s.t.) constraints (1)–(10),
$$Y_i \leq \bar{y}_i X_i, \quad \forall i \in \mathcal{I},$$

$$\phi_{ije} = 0, \quad \forall i,j \in \mathcal{I}, e < e^r_{ij} \quad \text{or} \quad e > e,$$

$$\psi_{ije} = 0, \quad \forall i,j \in \mathcal{I}, e < e_{ij} \quad \text{or} \quad e > e,$$

$$0 \leq \alpha_{ie} \leq 1, \ \forall i \in \mathcal{I}, e \in \mathcal{E},$$

$$Y_i, \phi_{ije}, \psi_{ije}, \lambda_{ie}, \eta_i, L_{ie}, Q_i \geq 0,$$

$$\forall i,j \in \mathcal{I}, e \in \mathcal{E},$$

$$X_i \in \{0,1\}, \ \forall i \in \mathcal{I}.$$

In this formulation, the objective is to maximize the operator's expected annual profit, which is the revenue from transit trips by customers net of the repositioning cost by workers and the investment in charging infrastructure. Vehicle flow rates  $(\psi, \phi, \lambda, \eta)$  and fixed costs (f,g) are all annualized. The additional constraint  $Y_i \leq \bar{y}_i X_i$  ensures that no charger will be installed without a charging site. As discussed in Section 3.1, the travel demand rates are time varying. We thus adopt the point-wise stationary approximation approach (Green and Kolesar 1991) to incorporate system dynamics over multiple periods. The detailed formulation for multiple periods is provided in Online Appendix B.

## 4. Solution Approach

Problem (NLP) is nonlinear and nonconvex owing to the fractional constraints (3)–(5) with quadratic terms that define queue lengths  $L_{ie}$  and  $Q_i$ . Fractional

constraints are common in queuing–location models but known to be difficult to tackle. In this section, we develop alternative formulations that are computationally efficient to solve. The idea is to overestimate (respectively, underestimate)  $L_{ie}$  and  $Q_e$  to generate a lower (respectively, upper) bound of the optimal (NLP) objective value.

#### 4.1. Lower Bound

To obtain a lower bound for (NLP), we first develop a transformation of  $L_{ie}$  into  $\hat{L}_{ie}$  in Lemma 1, and then we construct overestimates of  $\hat{L}_{ie}$  in Lemma 2 and those of  $Q_i$  in Lemma 3 as follows. We relegate the proofs and additional computational details to Online Appendix C.

**Lemma 1.** The average number of idle EVs waiting in zone i is given by

$$\sum_{e \in \mathscr{E}} L_{ie} = \sum_{e \in \mathscr{E}} \hat{L}_{ie}, \text{ where}$$

$$\hat{L}_{ie} = \begin{cases} 0, & \text{if } e = 0, \\ \frac{\left(\hat{d}_{ie} - \hat{d}_{i(e-1)}\right) \sum_{e' = e}^{\bar{e}} \frac{\alpha_{ie'}}{d\hat{q}_{ie'}}}{1 - \sum_{e' = e}^{\bar{e}} \alpha_{ie'}}, & \text{if } e = 1, \dots, \bar{e}. \end{cases}$$

$$(11)$$

Although  $L_{ie}$  is a ratio of quadratic terms in  $\alpha_{ie}$  in (3), Lemma 1 shows that  $\sum_{e \in \mathscr{C}} L_{ie}$  can be effectively simplified as a sum of linear ratios. When solving the optimization problem, we can safely rewrite the definition of  $\hat{L}_{ie}$  as

$$\hat{L}_{ie} \ge \begin{cases} 0, & \text{if } e = 0, \\ \frac{\left(\hat{d}_{ie} - \hat{d}_{i(e-1)}\right) \sum_{e'=e}^{\bar{e}} \frac{\alpha_{ie'}}{a_{ie'}}}{1 - \sum_{e'=e}^{\bar{e}} \alpha_{ie'}}, & \text{if } e = 1, \dots, \bar{e}. \end{cases}$$
(12)

**Lemma 2.** For any e > 0 and any constant  $\hat{m}_{ie} > 0$ , if  $\hat{L}_{ie}$  satisfies the constraint

$$\left(\hat{L}_{ie} + \left(1 - \sum_{e'=e}^{\bar{e}} \alpha_{ie'}\right)\right)^{2} \ge \frac{\left(\left(\hat{d}_{ie} - \hat{d}_{i(e-1)}\right) \sum_{e'=e}^{\bar{e}} \frac{\alpha_{ie'}}{\hat{d}_{ie'}} + \hat{m}_{ie}\right)^{2}}{\hat{m}_{ie}} + \left(\hat{L}_{ie} - \left(1 - \sum_{e'=e}^{\bar{e}} \alpha_{ie'}\right)\right)^{2}, \tag{13}$$

then  $\hat{L}_{ie}$  also satisfies the constraint (12).

**Lemma 3.** For any constants  $\hat{n}_i, \hat{w}_i > 0$ , if  $Q_i$  satisfies the constraints

$$\begin{cases}
\left(Q_{i} - \sum_{e < \bar{e}} \frac{\bar{e} - e}{u} \lambda_{ie} + Z_{i}\right)^{2} \\
\geq \left(\frac{\sum_{e < \bar{e}} \frac{\bar{e} - e^{2}}{\hat{n}_{i}} \lambda_{ie} + \hat{n}_{i} \sum_{e < \bar{e}} \lambda_{ie}}{u}\right)^{2} + \left(Q_{i} - \sum_{e < \bar{e}} \frac{\bar{e} - e}{u} \lambda_{ie} - Z_{i}\right)^{2}, \\
\left(2Y_{i} - \sum_{e < \bar{e}} \frac{\bar{e} - e}{u} \lambda_{ie}\right)^{2} \geq \frac{(Z_{i} + X_{i}\hat{w}_{i})^{2}}{2\hat{w}_{i}} \\
+ \left(\sum_{e < \bar{e}} \frac{\bar{e} - e}{u} \lambda_{ie}\right)^{2},
\end{cases} (14)$$

then  $Q_i$  also satisfies the modified constraint (5) with a replacement of the "=" sign with the " $\geq$ " sign.

Using the constraints from Lemmas 2 and 3, we provide a lower bound on the optimal objective value of (NLP) in the following proposition.

**Proposition 1.** A lower bound problem for (NLP) can be formulated as an MISOCP by replacing  $\sum_{e \in \mathscr{E}} L_{ie}$  with  $\sum_{e \in \mathscr{E}} \hat{L}_{ie}$  in (10) and replacing constraints (3)–(5) in (NLP) with constraints (13) and (14).

We call the resulting formulation (SOCP-LB). The formulation is an MISOCP because (13) and (14) can be converted into second-order cone (SOC) constraints in the standard two-norm form. For example, (13) is equivalent to

$$\hat{L}_{ie} + \left(1 - \sum_{e'=e}^{\bar{e}} \alpha_{ie'}\right) \ge \left\| \begin{pmatrix} \left(\hat{d}_{ie} - \hat{d}_{i(e-1)}\right) \sum_{e'=e}^{\bar{e}} \frac{\alpha_{ie'}}{d_{ie'}} + \hat{m}_{ie} \end{pmatrix} \middle/ \sqrt{\hat{m}_{ie}} \right\|_{2},$$

where the left-hand side is ensured to be nonnegative, as discussed in Online Appendix C. Meanwhile, all the other constraints and the objective function are linear in the decision variables. State-of-the-art software such as GUROBI provides standard solvers for MISOCP. For a comprehensive review of MISOCP, please also refer to Alizadeh and Goldfarb (2001). Because the optimal solution from (SOCP-LB) is a feasible solution to (NLP), the optimal objective value of (SOCP-LB) is no greater than that of (NLP).

#### 4.2. Upper Bound

To obtain an upper bound for (NLP), we underestimate  $\sum_{e \in \mathcal{E}} L_{ie}$  and  $Q_i$  in this subsection.

**Lemma 4.** If  $L_{ie}$  satisfies constraints (3) and (4) in (NLP), then  $\forall e^c \in \{1, 2, ..., \bar{e}\}, \ \Sigma_{e \in \mathscr{E}} L_{ie}$  satisfies the SOC-representable constraint

$$\left(\frac{\sum_{e \in \mathscr{E}} L_{ie} + 2 - \sum_{e=e^{c}}^{\bar{e}} \alpha_{ie}}{2}\right)^{2}$$

$$\geq \left(\frac{\sum_{e \in \mathscr{E}} L_{ie} + \sum_{e=e^{c}}^{\bar{e}} \alpha_{ie}}{2}\right)^{2} + \frac{\hat{d}_{e^{c}}}{\hat{d}_{\bar{e}}}.$$
(15)

Although inequality (15) is valid for all  $e^c \in \{1, 2, ..., \bar{e}\}$ , we only need to include a selection of  $e^c$  to avoid an excessive number of conic constraints, as discussed in Online Appendix C. We next underestimate  $Q_i$  by dropping the fractional term in constraint (5) as follows:

$$Q_i \ge \sum_{e < \bar{e}} \frac{\bar{e} - e}{u} \lambda_{ie}. \tag{16}$$

We then provide the upper bound for (NLP) in Proposition 2.

**Proposition 2.** The upper bound problem for (NLP) can be formulated as an MISOCP by replacing constraints (3)–(5) in (NLP) with constraints (15) and (16).

We call the resulting formulation (SOCP-UB). According to Lemma 4 and constraint (16), the optimal solution to (NLP) is a feasible solution to (SOCP-UB). Therefore, the optimal value of (SOCP-UB) is higher than that of (NLP).

The above-proposed lower bound (LB) and upper bound (UB) solution approach has three merits. First, the optimality gap between (SOCP-LB) and (SOCP-UB) is small, given adequate fleet size *m*, as tested in our case study. Second, this approach is computationally efficient. All numerical instances in our case study can be solved in less than 10 minutes (including parameter tuning for  $\hat{m}_{ie}$ ,  $\hat{n}_i$ , and  $\hat{w}_i$ ) using a personal laptop. Third, for EV-sharing practitioners, our MISOCP formulations are relatively straightforward to implement by calling a commercial solver. By contrast, state-of-the-art solution algorithms for the quadratic sum-of-ratios fractional programs problem, to which (NLP) reduces, are significantly more intricate. For example, the recent algorithm in Jiao and Liu (2017) involves an iterative procedure of linearization, branching, and bounding that can be elusive for tuning. Hence, we solve (SOCP-LB) for the feasible and near-optimal system design in our following case study.

## 5. Case Study and Managerial Implications

Based on the above-mentioned optimization model and the solution approach, this section discusses how to enhance the viability and profitability of EV sharing in practice. We first describe the setting of our case study and propose a design of charger deployment. Then we focus on answering five questions on different practical aspects of EV sharing:

- 1. How does the accuracy of our solution approach depend on fleet size and other system parameters?
- 2. Is there an economically efficient yet easy-toimplement charging policy?
- 3. Should EV sharing rely on a public or private charging network?
- 4. What are the implications of technology advancements?
- 5. How does urban spatial structure affect EV-sharing operations?

Finally, we validate our findings with the California Household Travel Survey for San Diego in Online Appendix Section D.4.

#### 5.1. Case Study: Car2go in San Diego

Our case study adopts an urban setting of 16 zip code zones in San Diego, California, where car2go ran an EV-sharing program in 2011–2016; it quit the San Diego market at the end of 2016. We identify 19,380 EV-sharing trips and 379 EVs from the data set, as described in Section 3.1. Additional information about the trips, charging sites, EV specifications, and cost

parameters are available in Online Appendix Section D.1.

One particular challenge in estimating trip demand is dealing with missing data. There are primarily two causes of the missing-data issue in our trip records: (1) the observed records were censored by vehicle availability and energy level because the demand was lost when there was no vehicle nearby with a sufficient energy level, and (2) occasionally, no information was received because of unstable application programming interface connections to the website. Therefore, we develop a convex optimization model and a tailored algorithm to recover the average demand based on the framework of tensor completion (e.g., Goldfarb and Qin 2014). The detailed procedure of demand estimation is provided in Online Appendix Section D.2.

In addition, we divide a day into five periods with different demand profiles, as described in Section 3.1. Hence, throughout the case study, we solve the multiperiod problem (provided in Online Appendix B) using our proposed solution approach developed in Section 4.

#### 5.2. Proposed Design and Operations

We solve the LB problem (SOCP-LB) to obtain the desired locations of charging sites, the associated number of chargers, and the EV flows of transit and repositioning trips at each energy level. By Proposition 1, the LB solution is a feasible solution to the original problem (NLP). Moreover, the LB solution is reasonably accurate: the LB profit from (SOCP-LB) is  $$1.62 \times 10^6$ , whereas the UB profit from (SOCP-UB) is  $$1.69 \times 10^6$ , implying a 4.19% optimality gap.

Our result suggests that the operator can serve 95.3% of the total demand by using only three charging sites with proactive repositioning activities. Figure 4 shows that our proposed design consists of three charging sites in zones 1, 7, and 14. The selected sites are either in or next to the zones with high demand flow volume (including both inflows and outflows). By having 40 chargers in zone 1, which is downtown San Diego, the operator can use the high traffic by customer trips to bring EVs to chargers. Zones 7 and 14 are both recommended to have 16 chargers such that these chargers are easily accessible from nearby zones in the west and east, respectively.

#### 5.3. Fleet Size and Bound Performance

The effectiveness of the proposed design and operations motivates us to examine several paths to improve EV-sharing-service operations in practice. First of all, we need to test the accuracy of the proposed solution approach for wide ranges of parameter values.

As shown previously, with 379 EVs in the car2go example, our proposed solution approach incurs an

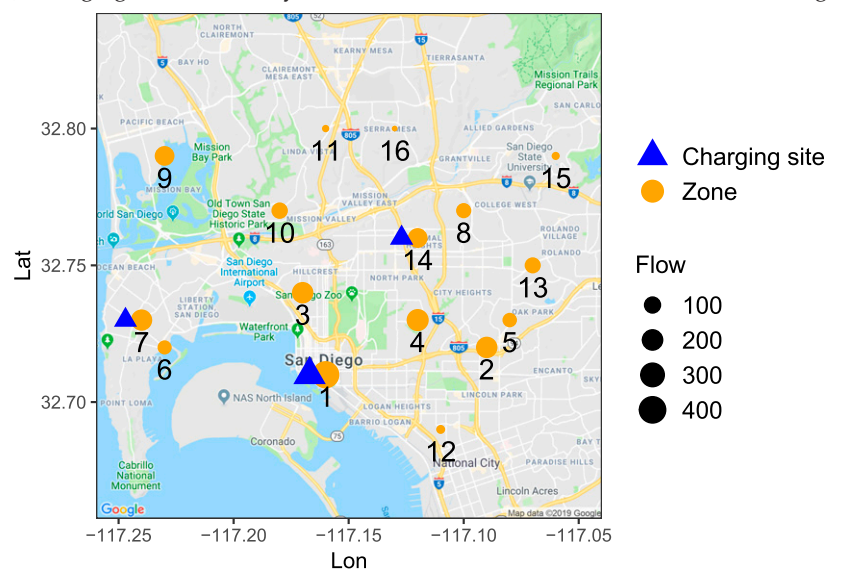


Figure 4. (Color online) Charging Sites and Daily Demand Flow Volume of Each Zone in San Diego

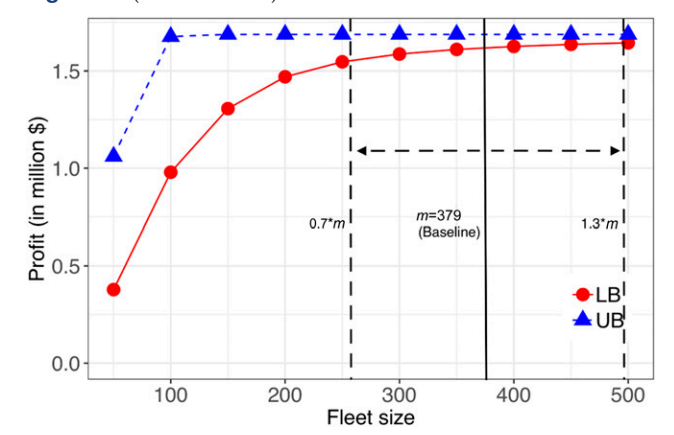
optimality gap of 4.19%. To further investigate the sensitivity of the bound performance with respect to fleet size, we vary fleet size and solve for both the LB and UB profits using (SOCP-LB) and (SOCP-UB) formulations. Figure 5 indicates that the optimality gap becomes reasonably small—less than 8% once the fleet size becomes at least 70% of the baseline level. Figure 5 also suggests that *car2go may have oversized its* EV fleet. A fleet size of 300, which is only 79.2% of the baseline size of car2go's fleet, is sufficient to generate more than 98.0% of the baseline LB profit (or 93.6% of the baseline UB profit). Both the LB and UB profits increase little if further adding EVs. The optimality gap widens when the fleet size drops below 70% of the baseline level, making it more difficult to infer the profitability. However, given the trip demand volume from the data, those scenarios are unrealistic because the fleet sizes deviate too much from the actual baseline level. We thus proceed to investigate other factors that affect car2go's performance. For all the numerical instances evaluated in Sections 5.4–5.7, the optimality gaps between the LB and UB profits are less than 5%, suggesting that the gap is insensitive to the variation of the other parameter values within the considered ranges. For example, the average optimality gaps are 3.7% for perturbing charging power, 4.2% for repositioning efficiency, 3.9% for battery capacity, and 4.5% for charger availability. We believe that this suboptimality is insignificant and does not mask our managerial insights.

## 5.4. Proactive vs. Threshold-Activated Charging-up-to Policies

We next show that car2go could have improved its charging operations. We examine the charging operations in the proposed solution by checking the energy levels of EVs. Figure 6(a) shows the energy-level distribution of EVs entering charging sites—that is,  $\sum_{i \in \mathcal{I}} \lambda_{ie}$  aggregated over all periods and then normalized into proportions with respect to each energy level e (here we evenly discretize the battery capacity into 15 energy levels with the charging-up-to level  $\bar{e} = 15$ ). The figure indicates that it is optimal to proactively charge EVs from varying energy levels. Such a proactive charging policy differs from car2go's practice of a threshold-activated charging policy—that is, charging EVs simply when their energy levels drop below the 20% threshold (recall Figure 3).

Despite its optimality, the proactive charging policy may be challenging for practitioners to implement. The threshold-activated charging policy, by contrast, is more implementable given its "single-parameter" simplicity. Therefore, we are interested in whether the EV-sharing service provider can keep employing a threshold-activated charging policy yet earn a

Figure 5. (Color online) LB and UB Profits in Fleet Size



higher profit simply by adjusting the charging activation threshold.

Interestingly, Figure 6(b) shows that the profit is remarkably sensitive to the threshold, peaking at 40% level. In other words, the operator may recover as much as 98.1% of the optimal profit with the proactive charging policy by raising the charging activation threshold from 20% to 40% (with the charging infrastructure reoptimized). In fact, both the 40% thresholdactivated charging policy and the proactive charging policy outperform the 20% threshold-activated charging policy because of two effects: (1) both policies boost the overall energy level of the fleet, and consequently, both policies increase the trip demands' fill rate, which is driven by the customer EV picking behavior, and (2) both policies improve the efficiency of repositioning operations as well as charger utilization; this is because either too low or too high a charging activation threshold incurs excessive repositioning trips for charging at suboptimal locations. Additional discussions on these effects are available in Online Appendix Section D.3. Proactive charging still generates a slightly higher profit than 40% threshold-activated charging because the former saves the repositioning cost by flexibly charging some EVs near a charging site before they hit the 40% threshold at farther locations. In sum, the EV-sharing-service provider may reap a near-optimal profit with a simple threshold-activated charging policy by carefully choosing the threshold level.

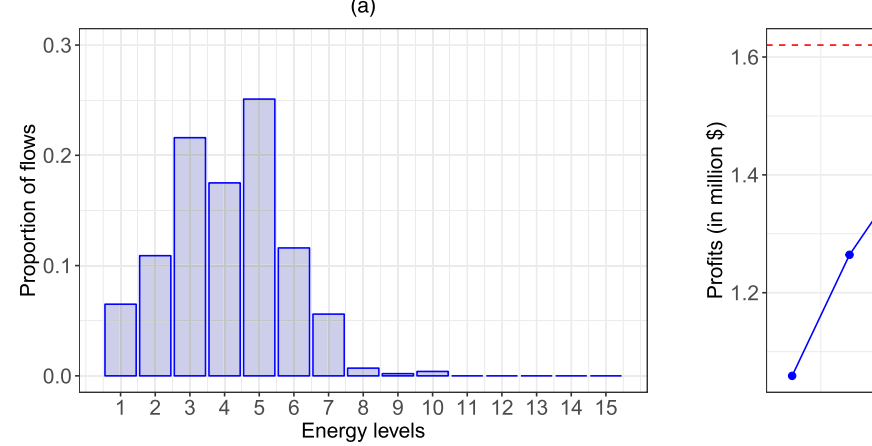
# 5.5. Private vs. Public Chargers: Location and Availability

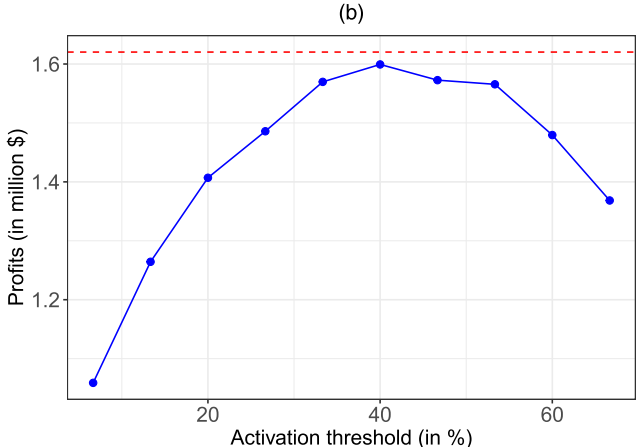
Clearly, building private charging sites incurs a heavy up-front investment. If the EV-sharing operator shoulders this cost, the charging sites should be economically deployed at optimal locations, as our proposed layout design shows. In reality, however, car2go relied on public chargers to power its EV fleet. The Department of Energy had promised to install 1,000 Blink chargers in San Diego through ECOtality. Unfortunately, ECOtality went bankrupt in 2013. Only about 400 chargers have been installed until recently. We find 386 public chargers, with their location information obtained from the U.S. Department of Energy (2017).

We thus investigate to what extent using public chargers at nonoptimized locations affects operating profits. A key challenge in using public chargers is that their availability is not guaranteed. This is because public chargers also face charging demands from other EV users. By contrast, the operator can enjoy 100% availability with private chargers. To illustrate the impact of charger availability on the trade-off between using public and private chargers, we consider two cases: (1) when using the public charging network, the operator has access to r% of the 386 public chargers at given locations, where r% is the average charger availability, and (2) when using a private charging network, the firm is able to optimize the allocation of an equivalent  $386 \times r\%$  number of chargers. In each case, we solve a modified version of (SOCP-LB) that ignores the fixed and variable charger investment costs and maximizes the operating profit. Figure 7 shows the operating profits at different levels of charger availability r% for both cases.

Figure 7 indicates that *charger availability is crucial to the operating profits when collaborating with a public charging network.* In particular, when the availability of the public charging network (e.g., ECOtality or Blink) is too low (< 25%), the associated operating profit is much lower than that from using private

Figure 6. (Color online) Comparison Between the Proactive Charging Policy and Threshold-Activated Charging Policies





*Note.* (a) Energy level distribution of EV flows (aggregated over all periods) entering charging sites under the proactive charging policy; (b) profits with different charging activation thresholds (dotted line) and the optimal profit with proactive charging (dashed line).

chargers because of the suboptimality of the charger locations. In that case, car2go should set up its own charging network (while also taking charger investment costs into account). If the public charging network increases the availability for car2go, the gap between the two operating profits narrows and eventually becomes insignificant. Therefore, this profit gap indicates the value of optimizing charger locations. With sufficient availability of public chargers, car2go should then rely on public chargers and focus on effectively repositioning EVs to charge at the right locations.

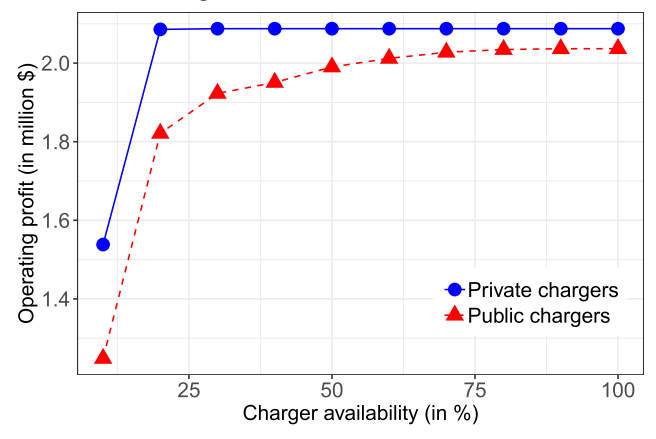
#### 5.6. Technological Advancements

EV-sharing operators are witnessing rapid advancements in EV technologies: First, the charging technology is maturing. The rated level 2 charging power is likely to increase to more than 19 kW, which is about six times the current 3.3 kW for car2go's Smart Electric Drive (Yilmaz and Krein 2013). Second, research and development in the energy density of the lithium-ion battery are making continuous progress, pointing to an EV future with a longer per-charge range (Blomgren 2017). Third, integrating autonomous vehicle technologies into the EV business is another intriguing prospect (Fehrenbacher 2016). Unmanned operations of EV repositioning and charging are expected to be significantly cheaper than using human labor.

Seeing the trends, we next examine how these technological advancements will impact EV-sharing-service operations. To this end, we perturb the values of charging power u, the battery energy capacity (or, equivalently, the highest energy level)  $\bar{e}$ , and the cost efficiency of vehicle repositioning  $\frac{1}{c}$ . Figure 8 shows the profit and total number of chargers in need in response to the parameter variations. We find that these technological factors throw impacts in different ways:

- Increasing the charging power significantly shortens the expected charging time and subsequently reduces the number of chargers needed. However, the profit increases only marginally because the main cost components such as the repositioning cost and site investment remain insignificantly affected.
- Increasing the battery capacity and the EV range increases the profit because doing so not only reduces the number of charging sites in need but also makes charging sites accessible at remote zones with lower fixed costs. With a longer range, repositioning trips for charging become less frequent and more flexible. Therefore, the repositioning cost also drops. By contrast, the impact on the number of chargers needed is indirect and insignificant. This is because the minimum charger quantity is determined by the total rate of electricity injection into the fleet. Given the charging power, this

**Figure 7.** (Color online) Operating Profits of Using Public and Private Chargers



injection rate depends on the total energy usage by transit and repositioning trips.

• Reducing the per-unit repositioning cost directly drives down the repositioning cost. Moreover, it allows building charging sites at less expensive locations without a significant increase in repositioning cost, although the repositioning trips become longer.

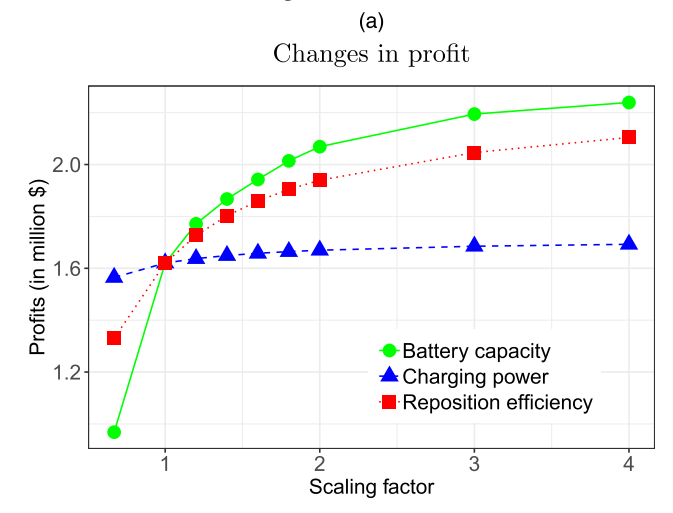
We summarize these observations into a twofold prescription: when chargers are limited in the early stage, the EV-sharing operator should first consider enhancing the charging power to alleviate its heavy dependence on charging infrastructure. When chargers become increasingly available, the operator should consider expanding battery capacity and reducing the repositioning cost to enhance its profitability.

#### 5.7. Urban Spatial Structure

We finally examine EV-sharing operations under more generic urban settings. As cities grow, they fill space naturally from the bottom up and/or by design from the top down, driven by a myriad of socioeconomic factors (Batty 2013). Consequently, cities differ in their centrality of spatial structures: Some cities are monocentric, where most of the activities are concentrated in the central business district, resulting in the outward ebb and inward flow of trips throughout a day. Other cities are more distributed and polycentric, resulting in trips with widespread origins and destinations (Louf and Barthelemy 2013).

To expand EV sharing in cities around the globe, we are interested in how EV-sharing-service operations are affected by urban spatial structure, particularly in terms of the centrality of the trip pattern. To formalize the notion of centrality, we adopt the definition of "start-to-complete networks" from the study by Bimpikis et al. (2019, p. 752) (which investigates a ride-sharing platform's pricing and compensation policies). Let matrix  $\mathbf{A}^{\xi}$  represent the trip pattern of a

**Figure 8.** (Color online) Impacts of Charging Power, Battery Capacity, and Repositioning Cost Efficiency on (a) the Profit and (b) the Number of Chargers Needed



Battery capacity
Charging power
Reposition efficiency

(b)

Changes in the number of chargers

city with n zones. For a trip originating from zone i, the element  $a_{ij}^{\xi}$  in  $\mathbf{A}^{\xi}$  is the probability that this trip will end at zone j. Moreover,  $\mathbf{A}^{\xi}$  is parameterized by  $\xi \in [0,1]$ :

$$\mathbf{A}^{\xi} = (1 - \xi)\mathbf{A}^D + \xi\mathbf{A}^C,$$

where

$$\mathbf{A}^{D} = \begin{bmatrix} 0 & 1/(n-1) & \cdots & 1/(n-1) \\ 1/(n-1) & 0 & \cdots & 1/(n-1) \\ \vdots & \vdots & \ddots & \vdots \\ 1/(n-1) & 1/(n-1) & \cdots & 0 \end{bmatrix}$$

and

$$\mathbf{A}^{C} = \begin{bmatrix} 0 & 1/(n-1) & \cdots & 1/(n-1) \\ 1 & 0 & \cdots & 0 \\ \vdots & \vdots & \ddots & \vdots \\ 1 & 0 & \cdots & 0 \end{bmatrix}.$$

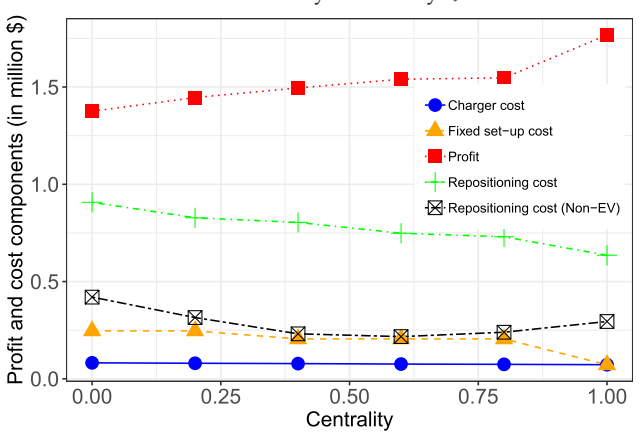
That is,  $\mathbf{A}^{\xi}$  is a convex combination of  $\mathbf{A}^D$  and  $\mathbf{A}^C$ , where  $\mathbf{A}^D$  represents the fully decentralized scenario in which all destinations are equally likely for a oneway trip from any origin, and  $\mathbf{A}^C$  represents the fully centralized scenario where zone 1, as the central district, is the only destination for all trips from other zones, and all trips from zone 1 are equally likely to end at any other zone. Hence,  $\xi$  captures urban spatial centrality: as  $\xi$  increases from 0 to 1, the trip pattern becomes more centralized around zone 1.

We use  $A^{\xi}$  to generate numerical instances with different degrees of centrality. Let  $d_i^k$  be the rate of customer trip demands originating from zone i in period k. We keep  $d_i^k$  the same as in our baseline setting but split  $d_i^k$  to each zone j according to  $d_{ij}^k = d_i^k a_{ij}^{\xi}$ . Then we solve (SOCP-LB) for six different values of centrality  $\xi$  ranging from 0 to 1.

Our results suggest that the EV-sharing operator may earn more profits as the urban centrality  $\xi$  increases. As Figure 9 shows, this profit increase is mainly attributable to the declining charging infrastructure cost and the declining repositioning cost. A higher degree of centrality, such as  $\xi = 1$ , as Figure 10(b) shows, would allow consolidating charging operations at the central district. Consequently, EV charging requires fewer charging sites and fewer chargers. The repositioning trips for charging are also shortened because the charging locations overlap more with customer trip origins and destinations. Conversely, a lower degree of centrality, such as  $\xi = 0$ , as Figure 10(a) shows, would entail building multiple charging sites at distributed locations with more chargers yet still incurring extra repositioning trips for charging at locations that are off customer trip routes.

The positive correlation between profitability and urban centrality highlights the importance of charging

**Figure 9.** (Color online) Profit and Cost Components in Demand Pattern Measured by Centrality  $\xi$ 



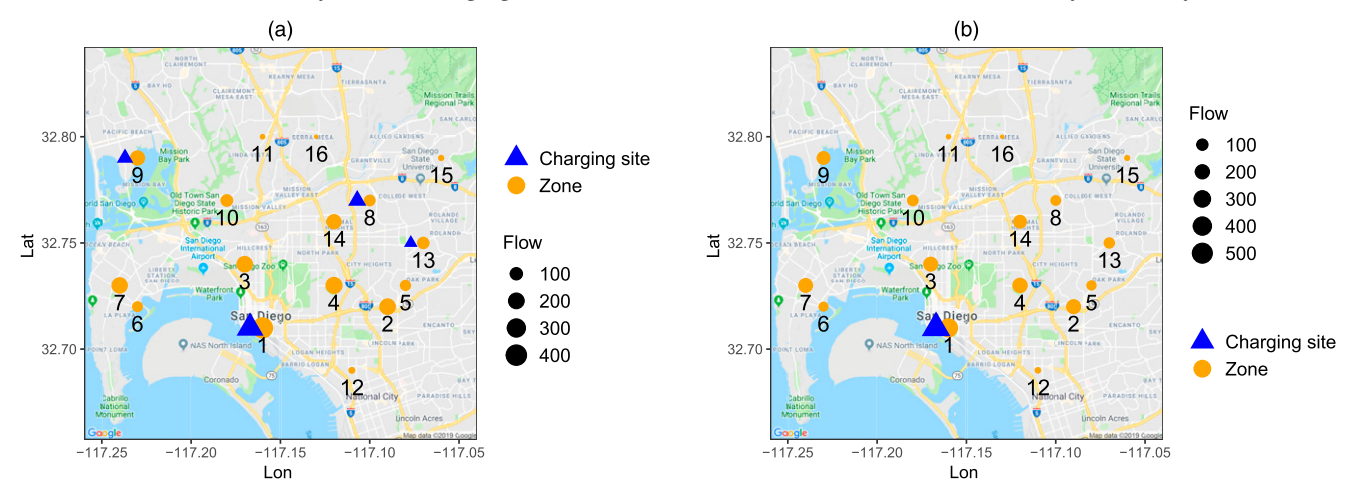


Figure 10. (Color online) Layouts of Charging Sites Under Different Demand Patterns Measured by Centrality  $\xi$ 

*Note.* (a) 83 chargers on 4 sites for centrality  $\xi = 0$ ; (b) 73 chargers on 1 site for centrality  $\xi = 1$ .

operations management. Consider, for comparison, a hypothetical vehicle-sharing system that involves no battery charging but otherwise resembles the system in our numerical setting. The relationship between centrality and the vehicle repositioning cost (only for rebalancing supply/demand) would become less obvious, as the black dash-dotted line in Figure 9 illustrates. As another comparison, for the ride-sharing system considered in Bimpikis et al. (2019) with no charging operations, the ride-sharing platform's profit is found to be even decreasing in centrality  $\xi$ . In their stylized setting, the demand rates  $d_i^k$  are assumed to be identical. As a result, centrality causes supply/ demand imbalances of the ride-sharing network. The platform has to use prices that are off the profitmaximizing level as an instrument to mitigate the imbalances. By contrast, our  $d_i^k$  from real data varies across locations and periods. Hence, the relationship between centrality and the expenditure on rebalancing supply/demand is less significant. Overall, our numerical results complement the discussion about trip pattern's impact on vehicle sharing in the literature—for EV sharing, the savings in charging operations and investment may dominate the expenditure on rebalancing supply/demand as urban centrality increases.

#### 6. Conclusion

This paper is motivated by a sheer gap: a smart city future where shared and electrified mobility prevails versus a reality where it may actually fail. To bridge this gap, we propose models, analytics, and insights for deploying a charging network and operating an EV-sharing system. In particular, we explicitly model a customer's endogenous usage of EVs at heterogeneous energy levels and the charging process under a charging-up-to policy. To deal with intractability in the resulting nonlinear optimization problem, we

develop both computationally efficient lower and upper bound problems as MISOCPs. We conduct a series of computational experiments using a set of real operational data.

Our case study on car2go's operations in San Diego leads to several findings. First, contrary to the practice of ECOtality, EV-sharing infrastructure planners should concentrate limited charging resources at selected optimal locations. If the EV-sharing operator collaborates with a public charging network, it is crucial to ensure charger availability to the EV-sharing fleet. Second, contrary to charging EVs only from energy levels of about 20%, car2go should either proactively charge EVs from varying energy levels or adjust the threshold to 40%. Either policy change can enhance the EV utilization rate, improve the repositioning efficiency, and subsequently significantly boost the profit. The operator should also carefully tailor its fleet size. Third, if technology permits, higher charging power can alleviate the dependence on scarce charging resources, whereas larger battery capacity or unmanned repositioning can improve profitability. Finally, the study on urban spatial structure again highlights the importance of charging planning and operations to EV sharing.

To further enhance the viability of shared and electrified mobility, several research challenges are worth confronting. For example, the infrastructure planning decisions are made up front in our setting. However, EV sharing is a fast-evolving business. It will be desirable to develop adaptive decision-making schemes for multistage infrastructure planning jointly with charging and repositioning operations. In addition, the prevalence of shared and electrified mobility will mean both burden and asset to the future urban electrical grid. Those grid implications also await further explorations. Finally, a dynamic yet implementable

charging policy (e.g., with time-varying charge-up-to levels) may also be investigated.

#### Acknowledgments

The authors gratefully acknowledge Professor Hau Lee, the associate editor, and three anonymous referees for their valuable comments that significantly improved this paper.

#### **Endnote**

<sup>1</sup> For more details, see https://www.smartnation.sg/ for Smart Nation Singapore, https://amsterdamsmartcity.com/ for Amsterdam Smart City, and https://www.columbus.gov/smartcolumbus/projects/ for Smart City Columbus (all accessed December 1, 2017).

#### References

- Abouee Mehrizi H, Baron O, Berman O, Chen D (2018) Adoption of electric vehicles in car sharing market. Working paper, University of Waterloo, Waterloo, ON, Canada.
- Adelman D (2007) Price-directed control of a closed logistics queueing network. *Oper. Res.* 55(6):1022–1038.
- Alizadeh F, Goldfarb D (2001) Second-order cone programming. *Math. Programming* 95(1):3–51.
- Baskett F, Chandy KM, Muntz RR, Palacios FG (1975) Open, closed, and mixed networks of queues with different classes of customers. J. ACM 22(2):248–260.
- Batty M (2013) The New Science of Cities (MIT Press, Cambridge, MA).Benjaafar S, Jiang D, Li X, Li X (2018) Inventory repositioning in ondemand product rental networks. Working paper, University of Minnesota, Minneapolis.
- Bimpikis K, Candogan O, Saban D (2019) Spatial pricing in ridesharing networks. *Oper. Res.* 67(3):744–769.
- Blomgren GE (2017) The development and future of lithium ion batteries. *J. Electrochemical Soc.* 164(1):A5019–A5025.
- Boyacı B, Zografos KG, Geroliminis N (2015) An optimization framework for the development of efficient one-way car-sharing systems. *Eur. J. Oper. Res.* 240(3):718–733.
- Condliffe J (2017) China and India want all new cars to be electric. MIT Tech. Rev. (September 11), https://www.technologyreview.com/the-download/608839/china-and-india-want-all-new-cars-to-be-electric/.
- Daley DJ (1976) Queueing output processes. Adv. Appl. Probab. 8(2): 395–415.
- Desaulniers G, Errico F, Irnich S, Schneider M (2016) Exact algorithms for electric vehicle-routing problems with time windows. *Oper. Res.* 64(6):1388–1405.
- Fehrenbacher K (2016) Future cities could run on shared fleets of electric self-driving cars. *Fortune* (October 11), http://fortune.com/2016/10/11/shared-electric-self-driving-cars/.
- Freund D, Henderson SG, O'Mahony E, Shmoys DB (2019) Analytics and bikes: Riding tandem with motivate to improve mobility. *INFORMS J. Appl. Analytics* 49(5):310–323.
- Garrick D (2016) Car2Go switching electric cars to gas. *San Diego Union-Tribune* (March 16), http://www.sandiegouniontribune.com/news/politics/sdut-car-share-car2go-fleet-gas-electric-2016mar16-story.html.
- George DK, Xia CH (2011) Fleet-sizing and service availability for a vehicle rental system via closed queueing networks. *Eur. J. Oper. Res.* 211(1):198–207.
- Goldfarb D, Qin Z (2014) Robust low-rank tensor recovery: Models and algorithms. SIAM J. Matrix Anal. Appl. 35(1):225–253.
- Green L, Kolesar P (1991) The pointwise stationary approximation for queues with nonstationary arrivals. *Management Sci.* 37(1):84–97.
- He L, Hu Z, Zhang M (2020) Robust repositioning for vehicle sharing. Manufacturing Service Oper. Management 22(2):241–256.

- He L, Mak H-Y, Rong Y, Shen Z-JM (2017) Service region design for urban electric vehicle sharing systems. Manufacturing Service Oper. Management 19(2):309–327.
- Jiang D, Powell W (2016) Practicality of nested risk measures for dynamic electric vehicle charging. Working paper, University of Pittsburgh, Pittsburgh.
- Jiao H, Liu S (2017) An efficient algorithm for quadratic sum-of-ratios fractional programs problem. *Numer. Funct. Anal. Optim.* 38(11): 1426–1445.
- Kabra A, Belavina E, Girotra K (2018) Bike share systems: Accessibility and availability. Chicago Booth Research Paper 15-04, Chicago Booth School of Business, Chicago.
- Kaspi M, Raviv T, Tzur M (2014) Parking reservation policies in oneway vehicle sharing systems. *Transportation Res. Part B: Meth-odological* 62(Suppl. C):35–50.
- Kaspi M, Raviv T, Tzur M, Galili H (2016) Regulating vehicle sharing systems through parking reservation policies: Analysis and performance bounds. Eur. J. Oper. Res. 251(3):969–987.
- Kim S-H, Whitt W (2014) Are call center and hospital arrivals well modeled by nonhomogeneous Poisson processes? *Manufacturing Service Oper. Management* 16(3):464–480.
- Kim SW, Mak H-Y, Olivares M, Rong Y (2018) Empirical investigation on the range anxiety for electric vehicles. Working paper, Chinese University of Hong Kong, Hong Kong.
- Kingman JFC (1965) The heavy traffic approximation in the theory of queues. Smith WL, Wilkinson WE, eds. Proc. Sympos. Congestion Theory (University of North Carolina Press, Chapel Hill), 137–159.
- Lim MK, Mak H-Y, Rong Y (2015) Toward mass adoption of electric vehicles: Impact of the range and resale anxieties. Manufacturing Service Oper. Management 17(1):101–119.
- Louf R, Barthelemy M (2013) Modeling the polycentric transition of cities. Phys. Rev. Lett. 111(19):198702-1-198702-5.
- Lu M, Chen Z, Shen S (2017) Optimizing the profitability and quality of service in carshare systems under demand uncertainty. *Manufacturing Service Oper. Management* 20(2):162–180.
- Mak H-Y, Rong Y, Shen Z-JM (2013) Infrastructure planning for electric vehicles with battery swapping. *Management Sci.* 59(7): 1557–1575.
- Nair R, Miller-Hooks E (2011) Fleet management for vehicle sharing operations. *Transportation Sci.* 45(4):524–540.
- Global Market Insights (2018) Car sharing market size by model (P2P, station-based, free-floating), by business model (round trip, one way), by application (business, private), industry analysis report, regional outlook, growth potential, competitive market share & forecast, 2018–2024. Accessed November 27, 2019, https://www.gminsights.com/industry-analysis/carsharing-market.
- Schneider M, Stenger A, Goeke D (2014) The electric vehicle-routing problem with time windows and recharging stations. *Transportation Sci.* 48(4):500–520.
- Shortle JF, Thompson JM, Gross D, Harris CM (2018) Fundamentals of Queueing Theory, 5th ed. (John Wiley & Sons, Hoboken, NJ).
- Shu J, Chou MC, Liu Q, Teo C-P, Wang I-L (2013) Models for effective deployment and redistribution of bicycles within public bicyclesharing systems. *Oper. Res.* 61(6):1346–1359.
- U.S. Department of Energy (2017) Alternative fuels data center. Accessed December 6, 2018, http://www.afdc.energy.gov/data\_download/.
- Whitt W (1993) Approximations for the *GI/G/m* queue. *Production Oper. Management* 2(2):114–161.
- Yilmaz M, Krein PT (2013) Review of battery charger topologies, charging power levels, and infrastructure for plug-in electric and hybrid vehicles. *IEEE Trans. Power Electronics* 28(5):2151–2169.
- Zhang H, Moura SJ, Hu Z, Qi W, Song Y (2018) A second-order cone programming model for PEV fast-charging station planning. *IEEE Trans. Power Systems* 33(3):2763–2777.